INFECTIOUS DISEASE

Paenibacillus infection with frequent viral coinfection contributes to postinfectious hydrocephalus in Ugandan infants

Joseph N. Paulson[1]*, Brent L. Williams[2,3]*, Christine Hehnly[4]*, Nischay Mishra[2,3]*, Shamim A. Sinnar[5,6]*, Lijun Zhang[4]*, Paddy Ssentongo[5,7,8]*, Edith Mbabazi-Kabachelor[9]*, Dona S. S. Wijetunge[10]*, Benjamin von Bredow[10]*, Ronnie Mulondo[9]*, Julius Kiwanuka[11]*†, Francis Bajunirwe[12], Joel Bazira[13], Lisa M. Bebell[14], Kathy Burgoine[15,16,17], Mara Couto-Rodriguez[2,18], Jessica E. Ericson[19], Tim Erickson[9], Matthew Ferrari[20,21,22], Melissa Gladstone[23], Cheng Guo[2], Murali Haran[22], Mady Hornig[3], Albert M. Isaacs[24], Brian Nsubuga Kaaya[9], Sheila M. Kangere[9], Abhaya V. Kulkarni[25], Elias Kumbakumba[11], Xiaoxiao Li[23], David D. Limbrick Jr.[26], Joshua Magombe[9], Sarah U. Morton[27], John Mugamba[9], James Ng[2], Peter Olupot-Olupot[16,28], Justin Onen[9], Mallory R. Peterson[5,7], Farrah Roy[29], Kathryn Sheldon[4], Reid Townsend[30], Andrew D. Weeks[31], Andrew J. Whalen[32], John Quackenbush[29‡], Peter Ssenyonga[9‡], Michael Y. Galperin[33‡], Mathieu Almeida[34‡], Hannah Atkins[35‡], Benjamin C. Warf[36‡], W. Ian Lipkin[2,3‡], James R. Broach[4‡], Steven J. Schiff[5,7,20,37,38‡§]

Postinfectious hydrocephalus (PIH), which often follows neonatal sepsis, is the most common cause of pediatric hydrocephalus worldwide, yet the microbial pathogens underlying this disease remain to be elucidated. Characterization of the microbial agents causing PIH would enable a shift from surgical palliation of cerebrospinal fluid (CSF) accumulation to prevention of the disease. Here, we examined blood and CSF samples collected from 100 consecutive infant cases of PIH and control cases comprising infants with non-postinfectious hydrocephalus in Uganda. Genomic sequencing of samples was undertaken to test for bacterial, fungal, and parasitic DNA; DNA and RNA sequencing was used to identify viruses; and bacterial culture recovery was used to identify potential causative organisms. We found that infection with the bacterium *Paenibacillus*, together with frequent cytomegalovirus (CMV) coinfection, was associated with PIH in our infant cohort. Assembly of the genome of a facultative anaerobic bacterial isolate recovered from cultures of CSF samples from PIH cases identified a strain of *Paenibacillus thiaminolyticus*. This strain, designated Mbale, was lethal when injected into mice in contrast to the benign reference *Paenibacillus* strain. These findings show that an unbiased pan-microbial approach enabled characterization of *Paenibacillus* in CSF samples from PIH cases, and point toward a pathway of more optimal treatment and prevention for PIH and other proximate neonatal infections.

[1]Department of Biostatistics, Product Development, Genentech Inc., South San Francisco, CA 94080, USA. [2]Center for Infection and Immunity, Mailman School of Public Health, Columbia University, New York, NY 10032, USA. [3]Department of Epidemiology, Columbia University Mailman School of Public Health, New York, NY 10032, USA. [4]Institute for Personalized Medicine, Department of Biochemistry and Molecular Biology, Pennsylvania State University College of Medicine, Hershey, PA 17033, USA. [5]Center for Neural Engineering, Pennsylvania State University, University Park, PA 16802, USA. [6]Department of Medicine, Pennsylvania State University College of Medicine, Hershey, PA 17033, USA. [7]Department of Engineering Science and Mechanics, Pennsylvania State University, University Park, PA 16802, USA. [8]Department of Public Health Sciences, Pennsylvania State University College of Medicine, Hershey, PA 17033, USA. [9]CURE Children's Hospital of Uganda, Plot 97-105, Bugwere Road, P.O. Box 903 Mbale, Uganda. [10]Department of Pathology, Pennsylvania State University College of Medicine, Hershey, PA 17033, USA. [11]Department of Pediatrics, Mbarara University of Science and Technology, P.O. Box 1410 Mbarara, Uganda. [12]Department of Epidemiology, Mbarara University of Science and Technology, P.O. Box 1410, Mbarara, Uganda. [13]Department of Microbiology, Mbarara University of Science and Technology, P.O. Box 1410 Mbarara, Uganda. [14]Division of Infectious Disease, Massachusetts Genereal Hospital, Harvard Medical School, 55 Fruit St, GRJ-504, Boston, MA 02114, USA. [15]Neonatal Unit, Department of Paediatrics and Child Health, Mbale Regional Referral Hospital, Plot 29-33 Pallisa Road, P.O. Box 1966, Mbale, Uganda. [16]Mbale Clinical Research Institute, Mbale Regional Referral Hospital, Plot 29-33 Pallisa Road, P.O. Box 1966 Mbale, Uganda. [17]University of Liverpool, Liverpool, L69 3BX, UK. [18]Biotia, 100 6th avenue, New York, NY 10013, USA. [19]Division of Pediatric Infectious Disease, Pennsylvania State University College of Medicine, Hershey, PA 17033, USA. [20]Center for Infectious Disease Dynamics, Pennsylvania State University, University Park, PA 16802, USA. [21]Department of Biology, Pennsylvania State University, University Park, PA 16802, USA. [22]Department of Statistics, Pennsylvania State University, University Park, PA 16802, USA. [23]Institute for Translational Medicine, University of Liverpool, Liverpool, L12 2AP, UK. [24]Department of Neuroscience, Washington University School of Medicine, St. Louis, MO 63130, USA. [25]Division of Neurosurgery, Hospital for Sick Children, University of Toronto, Toronto, Ontario, M5G 1X8, Canada. [26]Department of Neurological Surgery, Washington University School of Medicine, St. Louis, MO 63130, USA. [27]Division of Newborn Medicine, Boston Children's Hospital and Department of Pediatrics, Harvard Medical School, Boston MA 02115, USA. [28]Busitema University, Mbale Campus, Plot 29-33 Pallisa Road, P.O. Box 1966, Mbale, Uganda. [29]Department of Biostatistics, Harvard T.H. Chan School of Public Health, Boston, MA 02115, USA. [30]Department of Medicine, Washington University School of Medicine , St. Louis, MO 63130, USA. [31]Sanyu Research Unit, Liverpool Women's Hospital, University of Liverpool, Liverpool L8 7SS, UK. [32]Department of Mechanical Engineering, Pennsylvania State University, University Park, PA 16802, USA. [33]National Center for Biotechnology Information, National Library of Medicine, National Institutes of Health, Bethesda, MD 20894, USA. [34]Université Paris-Saclay, INRAE, MGP, Jouy-en-Josas, 78350, France. [35]Department of Comparative Medicine, Pennsylvania State University College of Medicine, Hershey, PA 17033, USA. [36]Department of Neurosurgery, Boston Children's Hospital, Harvard Medical School, Boston, MA 02115, USA. [37]Department of Neurosurgery, Pennsylvania State University College of Medicine, Hershey, PA 17033, USA. [38]Department of Physics, Pennsylvania State University, University Park, PA 16802, USA.
*These authors contributed equally to this work.
†Deceased.
‡These authors contributed equally to this work.
§Corresponding author. Email: steven.j.schiff@gmail.com

INTRODUCTION

Hydrocephalus is the most common indication for neurosurgery in children. Of the estimated 400,000 new cases each year, about half are estimated to be postinfectious, with the largest number of cases in low- and middle-income countries, especially sub-Saharan Africa (*1*). Neonatal sepsis (*2*) often precedes postinfectious hydrocephalus (PIH) (*3*), although the manifestations of hydrocephalus typically emerge in the months after the neonatal period as sufficient cerebrospinal fluid (CSF) accumulates such that cranial expansion garners medical attention. Thus, although these infants will typically die in early childhood without advanced surgical management, they are omitted from neonatal mortality surveillance (*4*).

The spectrum of microbial agents that underlie PIH remains poorly characterized. It is known that seasonal *Neisseria* epidemics can produce such cases within the African meningitis belt (*5*), and there have been reports of a tendency toward Gram-negative coliform bacteria in infants in other southern (*6*) and eastern (*7*) African locations where *Neisseria* is uncommon. A well-controlled examination of the pathogenic organisms underlying PIH needs to be conducted because it remains unclear what roles viruses, parasites, or fungi might play in addition to bacteria. If the microbial agents causing PIH were better characterized, then emphasis could shift from surgical palliation of CSF accumulation (*8*) to prevention of PIH.

In this study, we examined blood and CSF samples from 100 consecutive cases of PIH and control cases of non-postinfectious hydrocephalus (NPIH) in infants under 3 months of age at the CURE Children's Hospital of Uganda (CCHU) in Mbale, Uganda. Since 2001, this pediatric neurosurgical hospital has treated thousands of cases of PIH and NPIH, with nearly uniform negative recovery of putative pathogens through standard bacterial culture. Here, we conducted molecular analysis of high-quality blood and CSF samples and undertook comprehensive testing for bacterial, fungal, and parasitic DNA; genomic and RNA transcript sequencing for viruses; and extensive bacterial culture recovery for taxonomic identification, genome assembly, and virulence characterization.

Table 1. Demographics and clinical characteristics of the PIH and NPIH cohorts. PIH, postinfectious hydrocephalus; NPIH, non-postinfectious hydrocephalus.

Characteristics	All patients *n* = 100	PIH *n* = 64	NPIH *n* = 36
Age in days, mean (SD)	57 (24)	66 (17)	43 (27)
Sex			
Male (%)	51 (51)	35 (55)	16 (44)
Female (%)	49 (49)	29 (45)	20 (56)
Peripheral blood WBC [1.0 × 10^3]/μl, mean (SD)	10.3 (3.6)	11.0 (3.8)	8.8 (2.6)
CSF WBC/μl, mean (SD)*	30 (62)	45 (74)	5 (0.5)
Hemoglobin (g/dl), mean (SD)	11.5 (2.2)	10.7 (1.3)	13.0 (2.8)
Hematocrit %, mean (SD)	36.8 (7.4)	34.1 (4.1)	41.6 (9.3)
CT scan scoring (# and % in each category)†			
0	32 (33)	8 (25)	24 (69)
1	15 (15)	7 (11)	8 (23)
2	13 (13)	10 (16)	3 (8)
3	11 (11)	11 (17)	0 (0)
4	27 (28)	27 (43)	0 (0)
HIV exposure status (# and %)			
Yes	5 (5)	3 (5)	2 (6)
No	95 (95)	61 (95)	34 (94)

*n = 99. †n = 98.

RESULTS

Demographics and clinical characteristics of the infant cohort

Between March and November 2016, 115 consecutive infants with hydrocephalus were screened, and 15 were excluded for the following reasons: 8 did not receive parental consent, 6 lived outside of Uganda (South Sudan and Kenya), and 1 weighed less than 2.5 kg. A total of 100 patients 3 months of age or younger with hydrocephalus were enrolled in the study: 64 were diagnosed with PIH, and 36 were diagnosed with NPIH. PIH patients were older (66 days versus 43 days, $P < 0.0001$), had higher peripheral and CSF white blood cell (WBC) counts, and were more likely to be anemic (hemoglobin, 10.7 g/dl versus 13.0 g/dl; $P < 0.0001$) compared with NPIH patients (Table 1). Preoperative computed tomography (CT) scans were available for 98 subjects. Of these, the PIH group was more likely to have a higher CT scan score reflective of brain abscesses, calcifications, loculations, and debris than the NPIH group ($P < 0.0001$; Table 1 and fig. S1). There were no significant differences in gender and HIV exposure frequencies between the groups. The homes of PIH patients were concentrated within central and eastern Uganda, in a swampy plateau north of Lake Victoria, and south and north of the banks of Lake Kyoga, whereas NPIH patients were more uniformly distributed geographically ($P \leq 0.03$ by linear discrimination; fig. S2).

Before admission for hydrocephalus, 15 infants received antibiotic treatment; however, records detailing the antibiotic type used were only available for 2 of these 15 patients (gentamicin with ampicillin in one case and gentamicin with ceftriaxone in the other case). Three patients received antibiotics to treat active infections at the CCHU after admission (ceftriaxone with gentamicin in one case and ceftriaxone alone in the other two cases). Such antibiotic treatment is provided as adjunct care for abscess management (with drainage and irrigation of larger accessible abscesses) before more definitive surgical treatment of hydrocephalus with endoscopic third ventriculostomy or insertion of a ventriculoperitoneal shunt (*8*).

Detection of bacterial pathogens in infant CSF samples

For bacterial pathogen discovery, both Sanger sequencing of the 16*S* ribosomal DNA (rDNA) V1-V4 region and next-generation sequencing of V1-V2 and V4 regions were performed on fresh-frozen

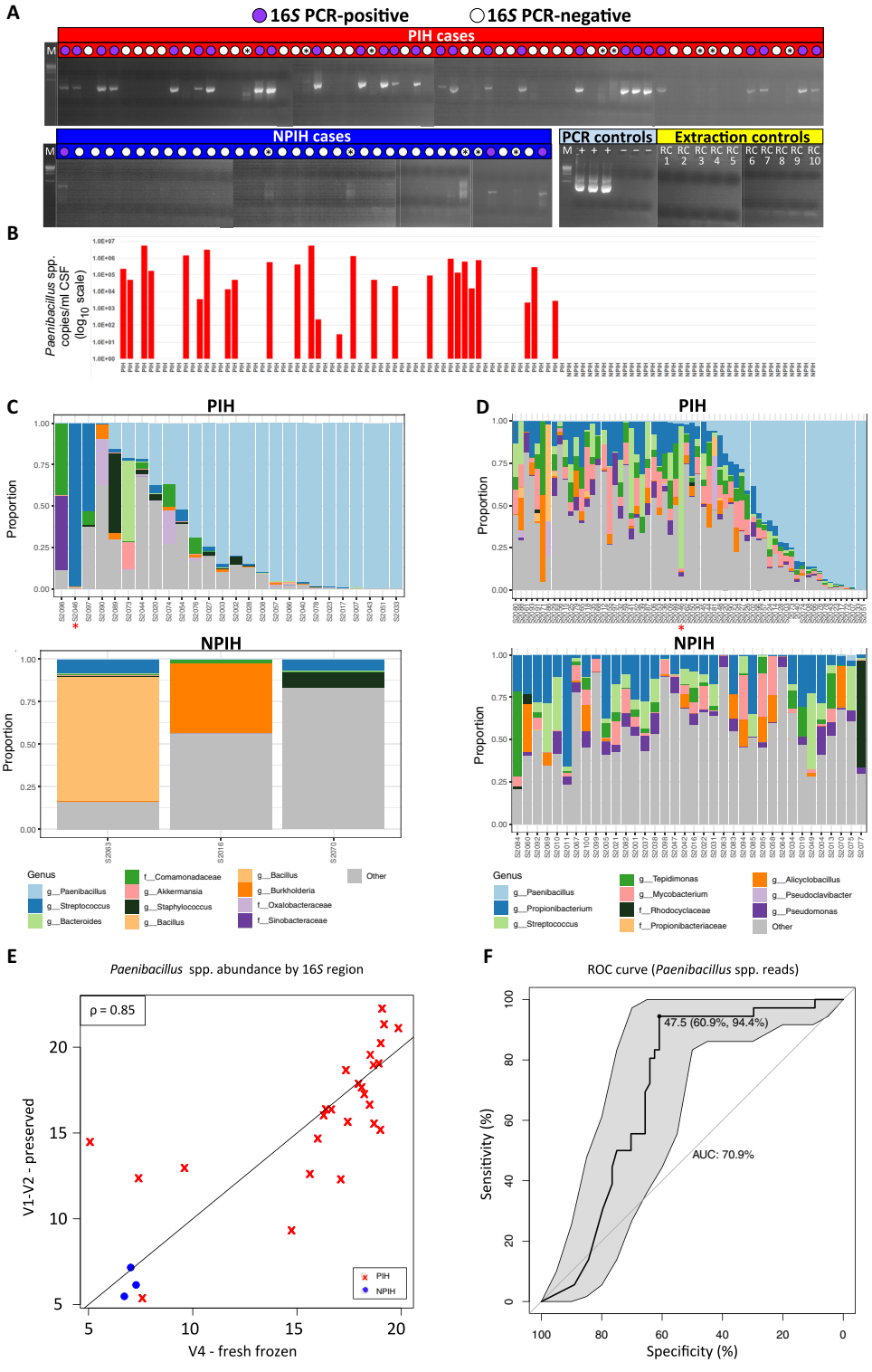

Fig. 1. 16S rDNA sequencing of PIH and NPIH CSF samples. (**A**) Agarose gels show 16*S* rDNA amplification products from CSF samples from patients with PIH (red) or NPIH (blue). Black asterisks denote lanes where faint nonspecific amplification (smears) or bands of unexpected sizes were observed. All amplification products including nonspecific amplifications were subjected to subcloning and sequencing. The following control samples were included: 10 negative extraction controls, 3 negative PCR controls (no template), and 3 positive PCR controls (DNA from human stool for bacteria or from soil for fungi). PCR-positive (+) and PCR-negative (–) controls (light blue) and 10 separate extraction reagent controls (RC) (yellow) are shown. Brightness and contrast were adjusted for gels to maximize visibility of faint bands and smears. (**B**) qPCR quantification of *Paenibacillus* spp. DNA in CSF samples from patients with PIH or NPIH. (**C** and **D**) Stacked bar relative abundance plots of the 16*S* rDNA V4 region (C) and the rDNA V1-V2 regions (D) for the most dominant bacterial taxa in PIH and NPIH CSF samples from (B) [in (C)] and for all 100 CSF samples (D). Red asterisks highlight a CSF sample from a patient with PIH who also had group B streptococcal infection. (**E**) Scatterplot of cumulative sum scaling–normalized *Paenibacillus* abundance: rDNA sequencing of fresh-frozen CSF samples (V4 region, abscissa) and preserved CSF samples (V1-V2 region, ordinate). Data points show normalized *Paenibacillus* abundance paired by patient ID for replicates of each patient sample. (**F**) Receiver operating characteristic (ROC) curve using the number of *Paenibacillus* reads as the predictor for PIH or NPIH status. Area under the curve (AUC) is 70.9% (95% DeLong CI = 60.6 to 81.2%). Sensitivity and specificity are maximized at 47.5 reads in a given sample, consistent with the threshold used for 50 reads.

and preserved CSF specimens in two different laboratories, which enabled us to account for known variation in microbial community amplicon sequencing (*9*) and to demonstrate the reproducibility of our findings.

Using DNA prepared from fresh-frozen CSF samples, conventional polymerase chain reaction (PCR) targeting of the V1-V4 16*S* rDNA gene region (table S1) revealed 16*S* rDNA amplification in CSF samples from 27 of 64 PIH cases but only 3 of 36 NPIH cases (Fig. 1A). V1-V4 Sanger sequencing of subcloned amplicons identified *Paenibacillus* as a predominant organism within the PIH cohort (23 of 64) but not within the NPIH cohort (0 of 36) (table S2). For quantification of *Paenibacillus* in CSF samples, *Paenibacillus* genus-specific quantitative PCR (qPCR) was performed, providing confirmation and quantification of 22 of the 23 CSF samples that were positive for *Paenibacillus* by Sanger sequencing and identifying 4 additional positive cases (Fig. 1B). Next-generation sequencing of the 16*S* rDNA V4 region was performed on all CSF samples from which amplification libraries could be obtained with composite MiSeq primers (26 of 64 PIH cases and 3 of 36 NPIH cases) (Fig. 1C). Only a few nucleotides distinguished

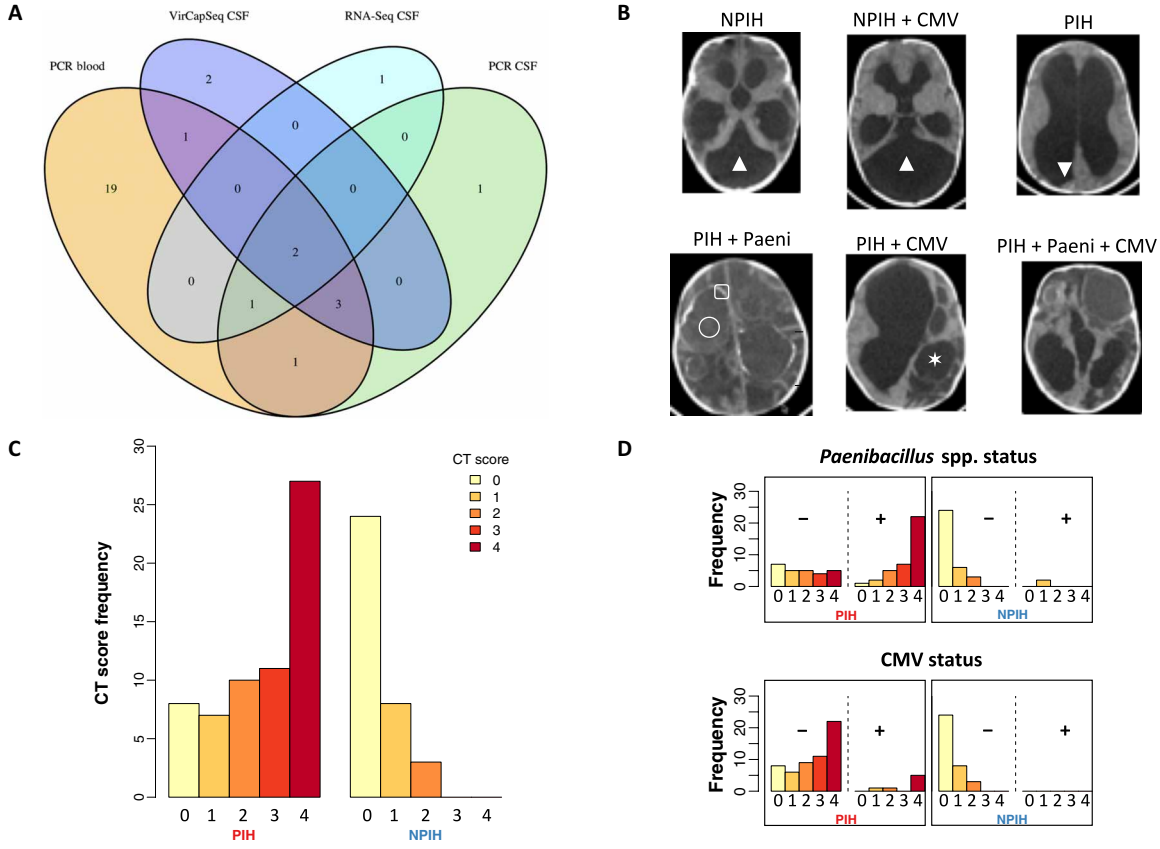

Fig. 2. CMV detection and CT brain imaging. (**A**) Venn diagram of CMV incidence detected using qPCR of blood samples or VirCapSeq, RNA sequencing (RNA-Seq) and real-time qPCR of CSF samples from patients with PIH or NPIH. (**B**) Representative CT brain images of patients with PIH or NPIH indicating infection with *Paenibacillus* (Paeni) or CMV. CT brain images for NPIH cases showed Dandy-Walker cyst malformations (white triangles) without a history or surgical findings of previous infection. In the PIH cases infected with *Paenibacillus*, notable brain abnormalities included multiple loculations of CSF (white star), higher-density fluid collections reflective of debris or blood within the CSF (inverted white triangle), ectopic calcification within the brain (white square), and abscess formation (white circle). (**C** and **D**) CT scores stratified by clinical indication (PIH or NPIH) (C) and as a function of CMV or *Paenibacillus* infection status (positive or negative) (D) (see also fig. S6).

Paenibacillus thiaminolyticus and *Paenibacillus popilliae* within the V1-V4 region, hindering species-level discrimination between these taxa. From the V1-V4 sequencing data, a phylogenetic tree was constructed, revealing that most of the *Paenibacillus* V1-V4 sequences were most closely related to *P. thiaminolyticus* and *P. popilliae*, with sequences from one individual with PIH most closely matching *Paenibacillus alvei* (fig. S3).

Using 16*S* rDNA from samples in DNA/RNA preservative, next-generation sequencing was performed on the V1-V2 region. Overall, representative sequences from the 1767 operational taxonomic units (OTUs) matched 159 genera. Most of the OTUs were sparsely represented except for a number of known skin flora, e.g., *Propionibacterium* spp. (Fig. 1D). More than half of the reads in 20% of the patients were attributed to the genus *Paenibacillus*. *Paenibacillus* spp. were present, defined as a minimum of 50 reads, in 38 PIH cases and 2 NPIH control cases (Fig. 1D).

To associate bacterial taxa with infection, we aggregated annotated OTUs at the genus level and performed differential abundance analysis. In performing linear regression analysis, *Paenibacillus* was the only genus associated with PIH after multiple testing correction (table S3). 16*S* rDNA abundance of *Paenibacillus* spp. was used as a marker for classifying patients with PIH and was consistent between V1-V2 and V4 regions (Fig. 1E). A receiver operating characteristic (ROC) analysis yielded an area under the curve (AUC) of 70.9% [95% DeLong confidence interval (CI) = 60.6 to 81.1%] for V1-V2 regions (Fig. 1F and fig. S4A), with an optimal threshold just below 50 reads. The geographical spatial distribution of PIH and PIH *Paenibacillus*-positive cases was significantly different from control NPIH cases ($P \leq 0.03$ and $P \leq 0.013$, respectively; fig. S2).

Other putative pathogens detected by 16*S* rDNA sequencing in CSF samples from individual cases at high abundance included sequences consistent with *Bacillus subtilis* and *Streptococcus agalactiae* (Fig. 1, C and D, and table S2). Bacterial diversity decreased as *Paenibacillus* abundance increased (fig. S4B). Most of the CSF samples had a similar microbial composition and β-diversity leading to no clear visual separation of PIH and NPIH cases when visualized with principal coordinates analysis (fig. S4C). Limiting OTU sequences to the set of OTUs annotated as *Paenibacillus* spp. revealed two or three clusters of patients with similar *Paenibacillus* abundance distributions (fig. S5). Further analysis of the microbial communities, including comparison of 16*S* rDNA regions and characterization of the taxonomy of bacterial isolates, is described in figs. S5 and S6 and table S3.

Detection of viral pathogens in infant CSF samples

Using the targeted viral detection capture technique VirCapSeq-VERT (*10*), we observed evidence of 11 viral strains distributed across

36% of the CSF samples: 32.8% of PIH cases and 41.6% of NPIH cases (table S4). Only cytomegalovirus (CMV) was abundant, which was confirmed by requiring positive findings on at least two replicates using two different qPCR methods (table S4) for all 100 preserved CSF and blood samples. CMV was confirmed in 27 of 100 patients including in 27 of 99 blood samples (18 of 64 PIH cases and 9 of 35 NPIH cases). However, CMV was found only in CSF samples (8 of 64 PIH and 0 of 36 NPIH) from PIH patients with CMV-positive blood samples (Fig. 2A). RNA sequencing data confirmed four cases of CMV infection by sequence matches to multiple mRNA transcripts, indicating the presence of replicating CMV (Fig. 2A). The geographical distribution of CMV-positive cases (PIH and NPIH combined) was not different from that for NPIH control cases (fig. S2).

Correlation of *Paenibacillus* with clinical signs of PIH

Several clinical measurements were positively associated with the presence of *Paenibacillus* including WBC counts in CSF and CT scan scores. In 12 months of follow-up, there were five deaths, three in the PIH cohort and two in the NPIH cohort. Each of the PIH deaths was in patients who were infected with *Paenibacillus*.

Scoring of brain CT scans based on the presence of brain abscesses, calcifications, loculations, and debris was calculated using preoperative images. PIH cases without measurable *Paenibacillus* infection had higher scores on the CT scans than did NPIH cases. PIH cases who were positive for *Paenibacillus* infection had higher CT scan scores compared to PIH cases who did not have *Paenibacillus* infection (Fig. 2, B and C; table S5; and figs. S1, S6, and S7). Each of the individual components of the CT score (abscesses, calcifications, loculations, and debris) was individually associated with PIH ($P < 10^{-5}$) or *Paenibacillus* ($P < 10^{-5}$) (table S5). All of the CSF samples that were positive for CMV were from PIH cases (table S6), and each of these PIH cases had at least one of the four signs comprising the CT scan score: six of seven fluid loculations, debris within fluid spaces, or ectopic calcification, and five of seven abscesses (table S7). We fitted an ordinal logistic regression model that included PIH versus NPIH status and presence of *Paenibacillus*. PIH cases had increased proportional odds for a high CT scan score with an odds ratio (OR; 95% CI) of 11.66 (4.29 to 33.94) and *Paenibacillus* presence with an OR (95% CI) of 7.6 (3.06 to 19.88). Testing for the presence of CMV did not show increased proportional odds of high CT scan scores (Fig. 2D) with an OR (95% CI) of 3.30 (0.52 to 29.66), when controlling for hydrocephalus etiology and the presence of *Paenibacillus*.

Paenibacillus spp. abundance was inversely correlated with patient age, consistent with residual sequelae after neonatal infection (Kruskal-Wallis, $P < 0.05$; Fig. 3A and fig. S6). Only PIH cases had high CSF WBC counts (>5/μl), and all were positive for *Paenibacillus* in the top abundance quartiles of normalized 16*S* rDNA counts (Fig. 3B and fig. S6). Infants with hydrocephalus may have considerable extra weight in their heads from CSF accumulation relative to their body mass. After calculating and subtracting excess fluid volume for age (*11*, *12*), we found no difference between this corrected weight for age with hydrocephalus and *Paenibacillus* status (Fig. 3C). Seizures were more commonly reported in patients with hydrocephalus before admission (25 versus 13) and during hospital admission (9 versus 1) if the patients were positive for *Paenibacillus*. The mean number of estimated days from initial febrile episode to when the head was noted to be growing was 21.4 ± 16.4 days versus 29.3 ± 25.4 days for *Paenibacillus*-positive versus *Paenibacillus*-negative cases. Blood in the CSF was noted in 15 CSF samples, but did not account for *Paenibacillus* positivity (1 of 7 *Paenibacillus*-positive PIH cases) or the presence of CMV in CSF (0 of 15 *Paenibacillus*-positive PIH or NPIH cases).

Characterization of *Paenibacillus* strains after recovery from CSF samples

From 600 initial cultures recovered from fresh-frozen CSF samples (table S8), 12 bacterial isolates were recovered from seven patients (table S9). Three *Paenibacillus* isolates were recovered from anaerobic blood culture bottles containing lytic liquid media (BD BACTEC): Two isolates subsequently grew on solid media after subculture, and a third *Paenibacillus* isolate failed to be subcultured on solid media and was identified directly from the liquid anaerobic

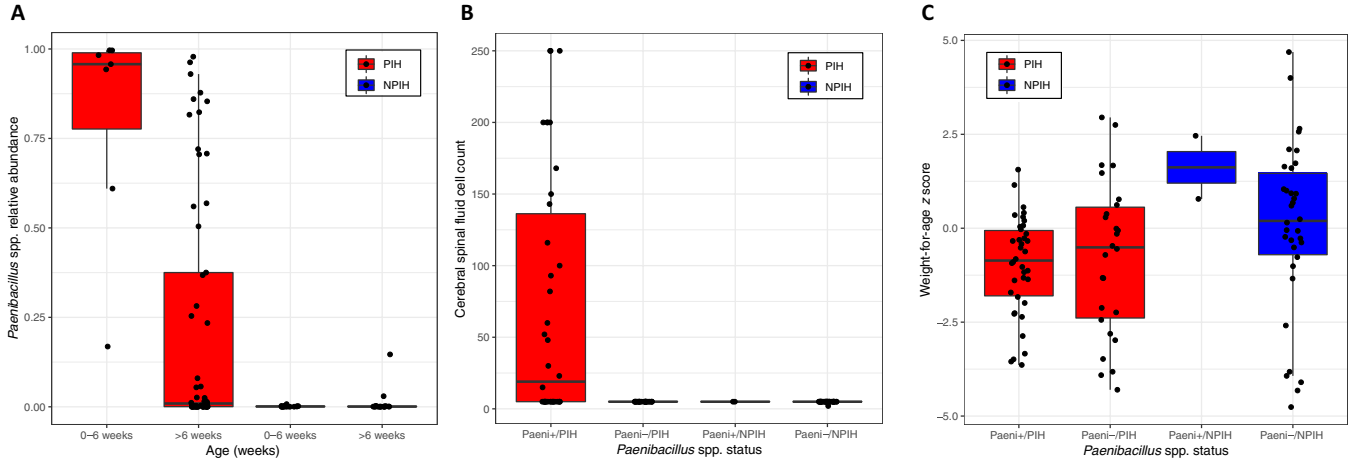

Fig. 3. Clinical signs associated with *Paenibacillus* infection. (**A**) Boxplots of $\log_2$-normalized *Paenibacillus* 16*S* rDNA abundance according to the age of patients with PIH or NPIH (categorized into 0 to 6 weeks and >6 weeks old) (see also fig. S6). (**B**) Boxplots of white blood cell (WBC) counts in CSF samples (cells per microliter) according to *Paenibacillus* infection (+/−) for patients with PIH or NPIH (see also fig. S6). Cell count values less than 5 were counted as 5. Cell count values greater than 250 were counted as 250. (**C**) Boxplots of corrected weight-for-age *z* scores according to *Paenibacillus* infection (+/−) for patients with PIH or NPIH, after calculating and subtracting excess CSF volume for age. Boxplots display the median and upper and lower quartiles, with whiskers indicating 1.5× the interquartile range.

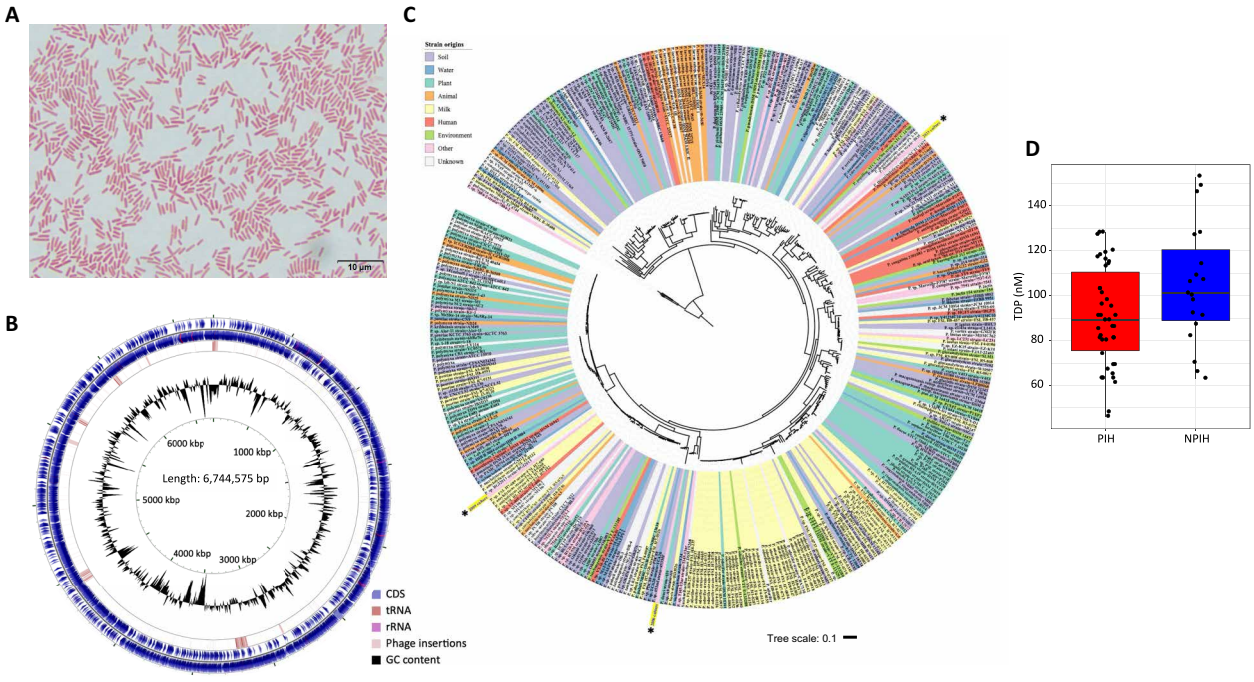

Fig. 4. Recovery of *P. thiaminolyticus* Mbale strain from PIH CSF samples after culture. CSF samples from three patients with PIH yielded three bacterial isolates after culture that were identified as *Paenibacillus* [black asterisks in (C)]. One isolate showed high 16*S* rDNA sequence identity to our V1-V2 and V4 region sequencing results. (**A**) Cultured *P. thiaminolyticus* Mbale strain stained with Gram stain at ×1000 magnification. Weak or negative Gram staining, despite a Gram-positive cell structure, is characteristic of *Paenibacillus* species (*53*). (**B**) To classify the *P. thiaminolyticus* clinical isolate, an extensive genome analysis was performed using both long-read and next-generation sequencing along with optical mapping. The resulting draft circular genome created using CGView, which features coding sequences (CDS), transfer RNA (tRNA), ribosomal RNA (rRNA), phage insertions, and GC content (53%), is shown. (**C**) Phylogenetic tree of *Paenibacillus* spp. based on 40 marker genes. The three bacterial isolates from cultured CSF samples are indicated by yellow tabs with black asterisks; isolate 2033 was renamed *P. thiaminolyticus* strain Mbale. (**D**) Concentrations (nM) of thiamine diphosphate (TDP) in blood samples from patients with PIH ($n = 42$) or NPIH ($n = 19$). TDP concentrations were lower in patients with PIH (*t* test, $P < 0.05$). Boxplots display the median and upper and lower quartiles, with whiskers indicating 1.5× the interquartile range. bp, base pair; kbp, kilo–base pair.

media. These three isolates were identified as *Paenibacillus* spp. using matrix-assisted laser desorption/ionization–time-of-flight (MALDI-TOF) mass spectrometry (table S9). Of the three inocula recovered, the two that grew on solid media after anaerobic liquid culture were identified as facultative anaerobes. Marker gene analysis of the three *Paenibacillus* isolates identified them as *P. thiaminolyticus*, *Paenibacillus amylolyticus*, and *Paenibacillus* sp. (Fig. 4). The 16*S* rDNA genes from the whole-genome sequences of the three isolates were compared to the representative 16*S* amplicon V1-V2 OTU cluster sequences. The *P. thiaminolyticus* isolate, one of the facultative anaerobes recovered, was most similar to that of OTU 99373, the most dominant OTU annotated as *Paenibacillus* in CSF samples from *Paenibacillus*-positive patients (fig. S5). This identified the *P. thiaminolyticus* strain (hereafter termed strain *Mbale*) as the isolate of interest for subsequent virulence testing in mice. We compared this strain by 16*S* rDNA gene similarity, average nucleotide identity (http://enve-omics.ce.gatech.edu/ani/) (*13*), and biochemical testing against the *P. thiaminolyticus* type strain NRRL B-4156^T (JCM 8360^T, GenBank accession CP041405). The 16*S* rDNA genes of this isolate had 99.2 to 99.4% identity, and the whole-genome average nucleotide identity (gANI) value was 97.06%, well above the 94 to 96% species threshold (*14*). Biochemical testing (https://apiweb.biomerieux.com; table S10) had a 99.5 to 99.9% identity, confirming that this isolate belonged to the *P. thiaminolyticus* species (*15*, *16*). Antibiotic sensitivity was tested, and the Mbale strain was found to be broadly sensitive to common antibiotics (table S11).

Because *P. thiaminolyticus* produces two thiaminases, we tested patient blood samples for thiamine deficiency. We assayed for thiamine diphosphate concentrations in whole blood and found that PIH cases (positive and negative for *Paenibacillus*) had lower thiamine diphosphate blood concentrations than did NPIH cases (*t* test, $P < 0.05$; Fig. 4D).

Pathogenicity of *Paenibacillus* strain Mbale

Comparative virulence of the *P. thiaminolyticus* Mbale strain was assessed using the reference strain NRRL B-4156 in age-matched C57BL/6J mouse littermates of both sexes, which were inoculated intraperitoneally at postnatal days 21 to 28. The reference strain demonstrated no adverse effects in the inoculated mice. In contrast, the Mbale strain produced sickness in all mice (16 of 16), with mortality or moribund states in 15 of 16 (93%) animals inoculated at a comparable concentration of colony-forming units (Fig. 5A and table S12). The Mbale strain produced acute tubular necrosis in the kidneys, myeloid hyperplasia in bone marrow, and moderate lymphocyte apoptosis in the splenic periarteriolar sheaths, but no notable brain lesions (Fig. 5B).

DISCUSSION

PIH may be the largest single cause of childhood hydrocephalus, which is the most common indication for neurosurgery in children worldwide. PIH cases are concentrated in low- and middle-income

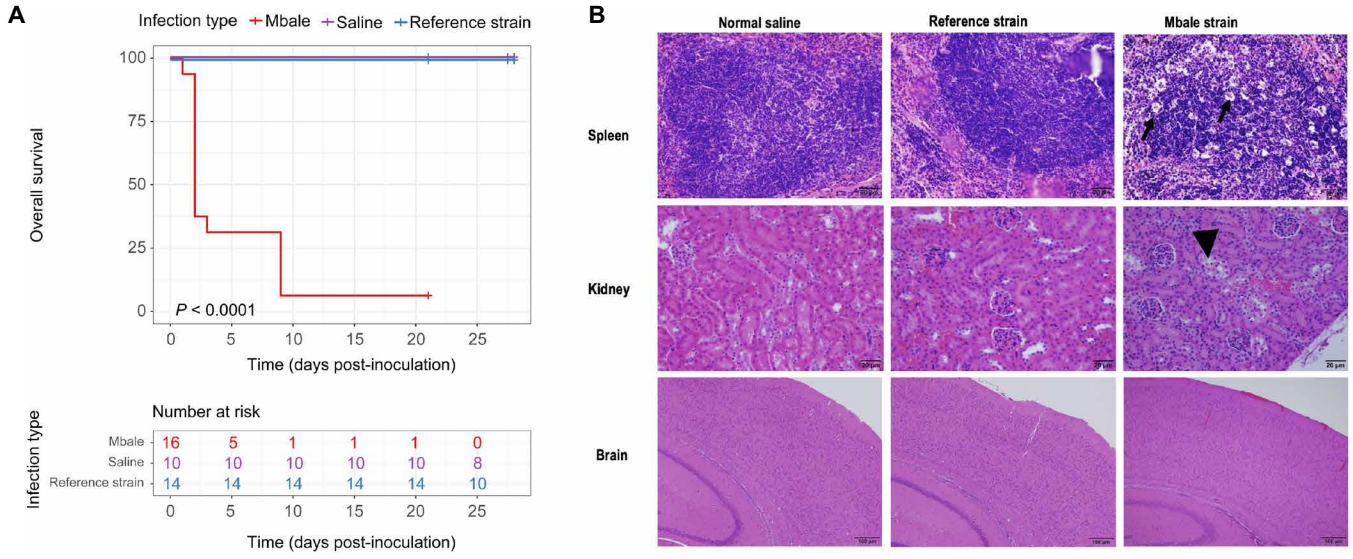

Fig. 5. Virulence testing of *P. thiaminolyticus* Mbale and reference strains in mice. Virulence of the *P. thiaminolyticus* Mbale strain and reference strain (NRRL B-4156^T) was assessed after intraperitoneal injection into postnatal day 21 to 28 C57BL/6J littermates, with an injection of saline as a control. (**A**) Kaplan-Meier survival curve for mice injected with Mbale strain (red), the reference strain (blue), or saline (purple). Mice injected with the *Mbale* strain had a worse overall survival (log-rank test, $P < 0.0001$). Mice injected with saline or the reference strain demonstrated no signs of illness and were euthanized at the end of the observation period. In contrast, mice receiving the Mbale strain at the same concentration as the reference strain (10^9 colony-forming units/ml) either died from infection on days 1 to 9, were euthanized because of a moribund state on days 2 and 3, or recovered from illness (one mouse that survived until euthanized on day 21). (**B**) Tissue sections were prepared from spleen, kidney, and brain of injected mice and stained with hematoxylin and eosin. Representative sections indicating no lesions in the spleen of mice inoculated with saline ($n = 6$) or the *P. thiaminolyticus* reference strain ($n = 10$) are shown. However, tingible body necrosis of macrophages (black arrows) containing intracytoplasmic apoptotic bodies was observed in the spleen sections from mice inoculated with the *P. thiaminolyticus* Mbale strain (9 of 10). There were no lesions in kidney sections from mice inoculated with saline or the *P. thiaminolyticus* reference strain, whereas pyknotic nuclei (black arrowhead) were observed in proximal tubule epithelial cells in kidney sections from mice inoculated with the *P. thiaminolyticus* Mbale strain (9 of 10) indicative of acute tubular necrosis. In mouse brain sections, there was no evidence of infection-associated pathology (saline control, $n = 6$ of 6; *P. thiaminolyticus* reference strain, $n = 10$ of 10; *P. thiaminolyticus* Mbale strain, $n = 10$ of 10).

countries (*1*), and the dominant predisposing event is often neonatal sepsis. Although PIH is, in principle, preventable, the microbial spectrum that accounts for this disease and the routes of infection are not well characterized. We have proposed that an unbiased identification of pathogens may be necessary to identify potential causal factors (*17*). PIH is part of a spectrum of conditions that, through activation of the immune system in the brain, lead to acquired hydrocephalus. The other major component of post-inflammatory hydrocephalus of infancy is intracerebral hemorrhage of prematurity. Both infection and hemorrhage within the brain lead to hydrocephalus through related inflammatory mechanisms (*18*). PIH is not a disease caused by a single organism; thus, use of an unbiased pan-microbial analysis in other parts of the world will likely reveal other organisms as important causes of PIH. One of the problems with using genomic techniques for pathogen detection from nominally sterile body fluids, such as blood and CSF, is that such low-biomass samples may have bacterial DNA contamination from reagents and other sources that can dominate the results (*19*), requiring substantial efforts such as statistical (*20*) and spike-in strategies (*21*) to reduce such effects. By using NPIH case-controls in our study consisting of contemporaneously recruited NPIH patients referred to the same hospital, we were able to rigorously contrast our analysis of infected samples from PIH patients to that of clinically uninfected control samples from NPIH patients. By replicating our bacterial discovery efforts on samples preserved differently in independent laboratories using separate regions of 16*S* rDNA, we obtained convergent results and demonstrated a dominant role for the pathogen *Paenibacillus* in our PIH infant cohort.

Whether previous analysis of PIH cases in Uganda was biased by reagent contamination is not known (*7*). We implemented several technical strategies to reduce the effect of background contamination. Despite contamination reduction efforts, the additional use of NPIH case-controls was critical to achieving convincing differences in pathogen abundance along with pathogen validation through recovery of bacteria in culture from CSF samples from PIH cases. The organism culture recovery rate was low, potentially due to the use of fresh-frozen CSF samples and administration of antibiotics to PIH cases before sampling.

Although various *Paenibacillus* spp. have been isolated occasionally from CSF (*22*–*24*), *P. thiaminolyticus* has not been known to be a virulent pathogen. It was first identified while screening for bacteria in the gut that might contribute to thiamine deficiency in people with beriberi in Asia (*25*). There is a single case report of in-dwelling catheter-associated *P. thiaminolyticus* bacteremia in an elderly patient on hemodialysis (*26*). This bacterium produces thiaminases I and II and is adapted to living in low-thiamine environments. Thiamine deficiency is associated with Wernicke's encephalopathy (*27*), two forms of beriberi (*28*), and polioencephalomalacia-associated brain necrosis in ruminant animals (*29*). In the developing world, thiamine deficiency is common in children (*30*) and is exacerbated by the stress of infection (*31*). Our findings demonstrate that thiamine was lower in children after infection regardless of infectious

etiology. Consistent with reports in animals (*32*), we did not find lower thiamine specifically due to infection with *P. thiaminolyticus*.

The underpinnings of *Paenibacillus* virulence are unclear. We found it difficult to culture this facultative anaerobe from clinical CSF samples. Once established in culture, the organism could be passaged using aerobic media. We speculate that, with a predilection to form calcified loculations and abscesses in the brain, *Paenibacillus* may have been growing anaerobically when sampled and may have required initial anaerobic culture conditions before being able to switch to aerobic metabolism. Alternatively, the lytic properties of the anaerobic broth used successfully in *Paenibacillus* recovery from CSF samples may have released viable organisms that were entrapped by intracellular phagocytosis within WBCs. In either case, *P. thiaminolyticus* acquired substantial virulence in comparison to the existing reference strain, as demonstrated by the almost complete lethality of *P. thiaminolyticus* when inoculated into mice compared to the reference strain. Supporting this increased virulence of *P. thiaminolyticus* are multiple phage insertions into its genome, and other protein coding and copy number variations, that await further characterization.

Although *P. thiaminolyticus* appears to be quite sensitive to common antibiotics, sufficient penetration of antibiotics into calcified abscesses to achieve adequate bactericidal concentrations is likely to be challenging. Ideally, such concentrations are achieved at initial point-of-care treatment for neonatal sepsis before infection of the brain. It is possible that within the immune-privileged brain (*33*), inadequate treatment during neonatal sepsis is a substantial factor in the persistent development of *P. thiaminolyticus* infection in the brain. How coinfection with CMV might affect disease severity in the setting of *P. thiaminolyticus* Mbale infection remains unclear. The typical clinical picture of these PIH cases is that of a brain ventriculitis without previous meningitis. Whether lumbar puncture in infants without meningeal infection could be diagnostic for *P. thiaminolyticus* during neonatal sepsis evaluation is unknown.

We found CSF purulence, a close match with *P. thiaminolyticus* DNA in CSF samples from our PIH infant cohort, and recovered *P. thiaminolyticus* from cultured CSF samples, yet demonstrating that *P. thiaminolyticus* causes PIH is likely to be more complex. Our analysis was limited to detection of active infections. For the geographical regions in which our group works, in utero exposure to infections by, for example, the malaria parasite is common (*34*). Predisposing in utero infections that are no longer active after birth (whether parasitic, viral, or bacterial) would remain undetected by our genomic sampling. Our finding of a substantial viral background infection with CMV cannot distinguish between congenitally acquired and postnatally acquired viral infection. The true incidence of in utero CMV infections in our PIH cohort was likely to have been higher than what we detected by testing several months after birth. In addition, our analysis does not address the heterogeneity in innate immunity (*35*) or nutritional status (*36*) among the infants in our PIH cohort, which are known to be predisposing factors for infection.

Our study has a number of other limitations. PIH is a syndrome, and although we identified a bacterial pathogen that appears to play a role in cases of PIH from eastern Uganda, it remains unclear whether this or other bacterial pathogens are associated with PIH in other regions of Africa and elsewhere. Whether *Paenibacillus* spp. predispose to invasion of the nervous system by CMV, or vice versa, remains unclear. We did not identify putative underlying bacterial causes of hydrocephalus in the 26 non-*Paenibacillus* PIH cases. A key limitation of our pan-microbial molecular approach may be the age of the patients because only survivors of neonatal sepsis develop PIH, and yet, the causative organisms need to be identified close in time to the original septic event. Analysis of the differences in virulence in mice inoculated with *P. thiaminolyticus* Mbale versus the reference strain was constrained by the rapid lethality of *P. thiaminolyticus* Mbale. This lethality, which may have been mediated by a bacterial toxin, could have precluded establishment of a brain infection, which is the hallmark of PIH. A limitation of our molecular study of disease causation is that the results, and our animal model, do not meet Koch's postulates for disease causation (*37*, *38*). Also, although *P. thiaminolyticus* Mbale strain was the dominant organism present in our PIH cases, there may have been other pathogens associated with PIH in our cohort that were not detected by our pan-microbial methods.

Our pan-microbial approach uncovered the presence of a difficult-to-grow pathogen, *P. thiaminolyticus* Mbale, not previously known to be virulent. This organism was associated with calcified loculations and brain abscesses in infants with PIH, as well as with hydrocephalus after survival from neonatal sepsis. The organism was present on a neurotropic viral background of CMV infection: 6 of 8 CSF samples and 11 of 27 blood samples from our PIH infant cohort were coinfected with CMV and *Paenibacillus* spp. Previous studies in adults in Uganda have reported that CMV viremia is frequently present in the setting of sepsis and is associated with increased risk of mortality (*39*–*41*). It has been hypothesized that immune modulation (*42*), rather than direct effects of CMV infection, is responsible for the association of CMV with worse outcomes in individuals with tuberculosis or cryptococcal meningitis. It is likely that, in many of these cases, latent CMV is reactivated when individuals become infected with another pathogen that alters the immune system's ability to keep the virus sequestered (*41*, *42*). Because of the ages of the infants in our PIH cohort (all <90 days of age), a majority of the CMV viremia we detected would be expected to come from primary CMV infection (acquired either congenitally or during early postnatal life) (*43*).

The demographics of *Paenibacillus* infection suggest localization to a circumscribed region in eastern Uganda. This is a region associated with the north and south banks of Lake Kyoga and the wetlands along the northern edge of Lake Victoria. It is characterized by large swamps and is a rice-growing region. Whether these infections are influenced by rainfall, which has been previously observed in PIH without pathogen identification (*44*), or share similarities with other environmental agents in similar topographies of the developing world (*45*) remains unknown.

Addressing the estimated 160,000 annual cases of PIH in the developing world (*1*), and the several million annual cases of neonatal sepsis (*2*), is a critical global health need. If a pan-microbial approach is required, then the current technology is neither readily scalable nor economically sustainable. However, the expansion of high-technology surgical facilities and pediatric neurosurgical care for patients with PIH is also not readily scalable (*46*). Long-term, less expensive, and more sustainable technologies to achieve pan-microbial surveillance in developing world settings, including maternal and environmental sources of infection, will be required to enable optimal treatment and, ultimately, prevention of neonatal infections and PIH.

MATERIALS AND METHODS

Study design

This study was conducted at the CCHU, a pediatric neurosurgical hospital in eastern Uganda that serves as a countrywide referral center

for patients with hydrocephalus. Infants were eligible for participation in the trial if they were 3 months of age or younger, met criteria for PIH or NPIH, and had a mother who was at least 18 years of age. The study was designed as a waste-fluid study at surgery with verbal consent. Ethics oversight was provided by the CCHU Institutional Review Board, the Mbarara University of Science and Technology Research Ethics Committee, and with oversight of the Ugandan National Council on Science and Technology. The study was approved by the Penn State University Institutional Review Board. A materials transfer agreement was in place between the CCHU and the Pennsylvania State University for the transfer of CSF and blood samples. A U.S. Centers for Disease Control and Prevention permit for the importation of infectious materials covered the transfer of specimens from the CCHU to Penn State University. An Institutional Biosafety Committee provided oversight of specimen handling at the Pennsylvania State University. A materials transfer agreement between the Pennsylvania State University and Columbia University covered the transport of materials between these research sites.

Inclusion criteria for PIH were as follows: age of 3 months or less, weight greater than 2.5 kg, no history consistent with hydrocephalus at birth, either a history of febrile illness or seizures preceding the onset of clinically apparent hydrocephalus or alternative findings (such as brain imaging and endoscopic results indicative of previous ventriculitis including septations, loculations, or deposits of debris within the brain ventricular system) (*3*), and finally mothers of at least 18 years of age who could give informed consent. Inclusion criteria for NPIH were as follows: age of 3 months or less, weight greater than 2.5 kg, findings of a noninfectious origin for hydrocephalus on CT brain scans or at endoscopy (e.g., lesions obstructing the aqueduct of Sylvius such as a tumor or cyst, aneurysm, or cavernous malformation, Dandy-Walker cyst, or other congenital malformation of the nervous system), or evidence of hemorrhage as a cause of hydrocephalus such as bloody CSF and absence of findings consistent with PIH or congenital origin of hydrocephalus, and mothers of at least 18 years of age who could give informed consent. Exclusion criteria were previous surgery on the nervous system (shunt, third ventriculostomy, or myelomeningocele closure) or evidence of communication of the nervous system with skin such as meningocele, encephalocele, dermal sinus tract, or fistula.

Sample collection and storage

Blood was sampled with aseptic technique at the time of surgery, either at the time of catheter placement for an intravenous line or during venipuncture for routine laboratory testing. CSF was obtained at the time of initial surgery. Many of the PIH cases were treated for abscess formation once or twice, before a definitive surgical procedure to address the hydrocephalus (endoscopic third ventriculostomy with choroid plexus cauterization or ventriculoperitoneal shunt insertion). Initial surgery might not have used an endoscope if the primary goal was aspiration and irrigation of purulent material from loculated fluid collections or frank abscesses. These initial procedures also might have included endoscopic lateral terminalis and septum pellucidum fenestrations. The endoscope was nearly universally used in all other cases, such as NPIH, as is our standard practice at this surgical site. Samples of blood and spinal fluid were divided into aliquots for fresh freezing or placement into DNA/RNA preservative (DNA/RNA Shield, Zymo Corporation), and specimens were frozen either at −80°C or placed in a liquid nitrogen Dewar or dry shipper. They were kept frozen through transport to the United States for further analysis. Thiamine diphosphate was quantified in frozen blood samples using high-performance liquid chromatography with tandem mass spectrometry at the Mayo Clinic Laboratories.

CT brain imaging

Preoperative CT brain scans were independently scored, blinded with respect to diagnosis, by two board-certified neurosurgeons who have considerable experience with infant hydrocephalus (B.C.W. and S.J.S.). One point was assigned for each of four possible findings: fluid loculations, debris within fluid spaces, ectopic calcifications within the brain parenchyma, and abscess formation. Discrepancies between scoring were then resolved with a consensus agreement.

Ribosomal RNA 16*S* gene sequencing

For characterization of bacterial species, we performed 16*S* rDNA amplicon sequencing. Separate CSF samples were sequenced at two different laboratories. Independent approaches were applied to limit background amplification of contaminants and decontaminate reagents (see the Supplementary Materials). At one laboratory, 16*S* amplicon sequencing of the V1-V4 region was performed on fresh-frozen samples using Sanger sequencing. Further next-generation amplicon metabarcode sequencing was performed on V4 for microbial background characterization, and *Paenibacillus* genus-specific qPCR for quantification was performed. At the other laboratory, a primer extension technique for 16*S* amplicon next-generation sequencing of the V1-V2 region on DNA/RNA preserved samples was performed. Using results from these two laboratories, 16*S* amplicon (regions V1-V2 and V4) reads sequenced from fresh-frozen CSF and preservative samples were clustered at 97% similarity (*47*). For downstream analyses, we accounted for sequencing variability using cumulative sum scaling–normalized taxa abundances (*48*). A primer table is given in table S1.

Pathogen characterization

Targeted PCR was performed in an attempt to detect the presence of Zika virus, chikungunya virus, human papillomavirus, parvovirus B19, toxoplasmosis, trypanosomiasis, malaria, and fungi (table S1). A broad screen for viral presence was performed in two different ways: VirCapSeq oligomer concentration (*10*) and total RNA sequencing analysis. For the viruses that appeared abundant in either PIH or NPIH, PCR confirmation was performed.

In an attempt to culture the putative pathogen, 100 fresh-frozen CSF samples were subjected to six different media outlined in table S8. If colonies grew on solid media, Gram stain and MALDI-TOF were performed to characterize the organism. For isolates identified as *Paenibacillus*, antibiotic sensitivity, biochemical testing, and whole-genome sequencing were performed.

A hybrid method was used to reconstruct the genome of a *P. thiaminolyticus* isolate, combining short-read sequencing, optical mapping (Bionano Genomics), and nanopore long contiguous sequencing (MinION, Oxford Nanopore Technologies). From the resulting whole-genome sequences and optical mapping assembly, a hybrid scaffold was generated (Bionano Hybrid Scaffold v1025201). For *P. amylolyticus* and *Paenibacillus* spp. isolates and reference type strain *P. thiaminolyticus* NRRL B-4156 (Agricultural Research Service Culture Collection, https://nrrl.ncaur.usda.gov/cgi-bin/usda/prokaryote/report.html?nrrlcodes=B-4156), only short-read and nanopore sequencing were used for assembly.

Virulence testing in mice

All animal experiments were performed with oversight by the Pennsylvania State University Institutional Animal Care and Use Committee and with Institutional Biosafety Committee approval at biosafety level 2 (BSL2). Virulence testing was performed on weanling postnatal day 21 to 28 C57BL/6J mice using up to 10^9 colony-forming units suspended in 100 μl of saline, or saline only, injected into the peritoneum. Bacteria for injection were thawed and subcultured before each inoculation and quantified using standard colony-forming unit methods (see the Supplementary Materials). Animals were humanely euthanized with CO_2 if they developed altered or depressed mentation or lost more than 20% of their body weight. A full complement of tissues was collected from each mouse by following the guidelines set forth by international veterinary toxicology interest groups (*49*–*51*). Tissues were preserved in 10% neutral buffered formalin, embedded in paraffin blocks, cut into 3-μm sections, and stained with hematoxylin and eosin for analysis. All organs were evaluated by a veterinary pathologist (H.A.).

Statistical analysis

Continuous demographic variables were evaluated using the nonparametric Wilcoxon rank sum (two-group comparisons) and Kruskal-Wallis (more than two group comparisons) tests following Shapiro-Wilk's test for normality, unless otherwise stated. Fisher's exact test was performed for categorical variables. All tests were two-sided unless stated otherwise. Ordinal logistic regression was applied to estimate the proportional odds of CT scan scores between indication, *Paenibacillus* presence or absence, and CMV status. We performed differential abundance analysis of taxa between PIH and NPIH groups and accounted for multiple testing leveraging a false discovery rate analysis (*52*).

SUPPLEMENTARY MATERIALS

stm.sciencemag.org/cgi/content/full/12/563/eaba0565/DC1
Materials and Methods
Fig. S1. CT brain scans for PIH and NPIH cases.
Fig. S2. Geographic location and spatial statistics of cases.
Fig. S3. Phylogenetic tree for 16*S* rDNA V1-V4 sequences.
Fig. S4. Further analysis of the microbial 16*S* rDNA community.
Fig. S5. Operational taxonomic unit heatmaps for *Paenibacillus*.
Fig. S6. Quantity of *Paenibacillus* in CSF by qPCR versus age, CT score, and WBC counts.
Fig. S7. CT scores as a function of CMV infection status.
Table S1. PCR primer table.
Table S2. qPCR and 16*S* rDNA sequencing of CSF samples.
Table S3. Differential abundance of V1-V2 rDNA sequencing data.
Table S4. Analysis of virus frequency using VirCapSeq, PCR, and RNA sequencing.
Table S5. Demographics of PIH and NPIH cases with or without *Paenibacillus* infection.
Table S6. *Paenibacillus* and CMV coinfection status.
Table S7. CT score versus CMV infection.
Table S8. Culture media composition.
Table S9. Results of culture recovery.
Table S10. Biochemical testing of *P. thiaminolyticus*.
Table S11. Antibiotic resistance testing of *P. thiaminolyticus* and *Paenibacillus* spp.
Table S12. Testing of *P. thiaminolyticus* virulence in mice.
References (*54*–*100*)

View/request a protocol for this paper from *Bio-protocol*.

REFERENCES AND NOTES

1. M. C. Dewan, A. Rattani, R. Mekary, L. J. Glancz, I. Yunusa, R. E. Baticulon, G. Fieggen, J. C. Wellons III, K. B. Park, B. C. Warf, Global hydrocephalus epidemiology and incidence: Systematic review and meta-analysis. *J. Neurosurg.* , 1–15 (2018).
2. S. L. Ranjeva, B. C. Warf, S. J. Schiff, Economic burden of neonatal sepsis in sub-Saharan Africa. *BMJ Glob. Health* **3**, e000347 (2018).
3. B. C. Warf, Hydrocephalus in Uganda: The predominance of infectious origin and primary management with endoscopic third ventriculostomy. *J. Neurosurg.* **102**, 1–15 (2005).
4. B. C. Warf, B. C. Alkire, S. Bhai, C. Hughes, S. J. Schiff, J. R. Vincent, J. G. Meara, Costs and benefits of neurosurgical intervention for infant hydrocephalus in sub-Saharan Africa. *J. Neurosurg. Pediatr.* **8**, 509–521 (2011).
5. I. A. Aziz, Hydrocephalus in the Sudan. *J. R. Coll. Surg. Edinb.* **21**, 222–224 (1976).
6. L. C. Handler, M. G. Wright, Postmeningitic hydrocephalus in infancy. Ventriculography with special reference to ventricular septa. *Neuroradiology* **16**, 31–35 (1978).
7. L. Li, A. Padhi, S. L. Ranjeva, S. C. Donaldson, B. C. Warf, J. Mugamba, D. Johnson, Z. Opio, B. Jayarao, V. Kapur, M. Poss, S. J. Schiff, Association of bacteria with hydrocephalus in Ugandan infants. *J. Neurosurg. Pediatr.* **7**, 73–87 (2011).
8. A. V. Kulkarni, S. J. Schiff, E. Mbabazi-Kabachelor, J. Mugamba, P. Ssenyonga, R. Donnelly, J. Levenbach, V. Monga, M. Peterson, M. MacDonald, V. Cherukuri, B. C. Warf, Endoscopic treatment versus shunting for infant hydrocephalus in Uganda. *N. Engl. J. Med.* **377**, 2456–2464 (2017).
9. R. Sinha, G. Abu-Ali, E. Vogtmann, A. A. Fodor, B. Ren, A. Amir, E. Schwager, J. Crabtree, S. Ma; Microbiome Quality Control Project Consortium, C. C. Abnet, R. Knight, O. White, C. Huttenhower, Assessment of variation in microbial community amplicon sequencing by the Microbiome Quality Control (MBQC) project consortium. *Nat. Biotechnol.* **35**, 1077–1086 (2017).
10. T. Briese, A. Kapoor, N. Mishra, K. Jain, A. Kumar, O. J. Jabado, W. I. Lipkin, Virome capture sequencing enables sensitive viral diagnosis and comprehensive virome analysis. *MBio* **6**, e01491-15 (2015).
11. M. Peterson, B. C. Warf, S. J. Schiff, Normative human brain volume growth. *J. Neurosurg. Pediatr.* **21**, 478–485 (2018).
12. J. G. Mandell, J. W. Langelaan, A. G. Webb, S. J. Schiff, Volumetric brain analysis in neurosurgery: Part 1. Particle filter segmentation of brain and cerebrospinal fluid growth dynamics from MRI and CT images. *J. Neurosurg. Pediatr.* **15**, 113–124 (2015).
13. R. L. Rodriguez-R, S. Gunturu, W. T. Harvey, R. Rosselló-Mora, J. M. Tiedje, J. R. Cole, K. T. Konstantinidis, The Microbial Genomes Atlas (MiGA) webserver: Taxonomic and gene diversity analysis of *Archaea* and *Bacteria* at the whole genome level. *Nucleic Acids Res.* **46**, W282–W288 (2018).
14. C. Hehnly, L. Lijun Zhang, J. Paulson, M. Almeida, B. von Bredow, D. S. S. Wijetunge, N. D. Olson, M. Galperin, K. Sheldon, S. J. Schiff, J. R. Broach, Complete genome sequences of the human pathogen *Paenibacillus thiaminolyticus* Mbale and type strain *P. thiaminolyticus* NRRL B-4156. *Microbiol. Resour. Announc.* **9**, e00181-20 (2020).
15. K. T. Konstantinidis, J. M. Tiedje, Genomic insights that advance the species definition for prokaryotes. *Proc. Natl. Acad. Sci. U.S.A.* **102**, 2567–2572 (2005).
16. J. Goris, K. T. Konstantinidis, J. A. Klappenbach, T. Coenye, P. Vandamme, J. M. Tiedje, DNA–DNA hybridization values and their relationship to whole-genome sequence similarities. *Int. J. Syst. Evol. Microbiol.* **57**, 81–91 (2007).
17. J. Kiwanuka, J. Bazira, J. Mwanga, D. Tumusiime, E. Nyesigire, N. Lwanga, B. C. Warf, V. Kapur, M. Poss, S. J. Schiff, The microbial spectrum of neonatal sepsis in Uganda: Recovery of culturable bacteria in mother-infant pairs. *PLOS ONE* **8**, e72775 (2013).
18. J. K. Karimy, B. C. Reeves, E. Damisah, P. Q. Duy, P. Antwi, W. David, K. Wang, S. J. Schiff, D. D. Limbrick Jr., S. L. Alper, B. C. Warf, M. Nedergaard, J. M. Simard, K. T. Kahle, Inflammation in acquired hydrocephalus: Pathogenic mechanisms and therapeutic targets. *Nat. Rev. Neurol.* **16**, 285–296 (2020).
19. S. J. Salter, M. J. Cox, E. M. Turek, S. T. Calus, W. O. Cookson, M. F. Moffatt, P. Turner, J. Parkhill, N. J. Loman, A. W. Walker, Reagent and laboratory contamination can critically impact sequence-based microbiome analyses. *BMC Biol.* **12**, 87 (2014).
20. N. M. Davis, D. M. Proctor, S. P. Holmes, D. A. Relman, B. J. Callahan, Simple statistical identification and removal of contaminant sequences in marker-gene and metagenomics data. *Microbiome* **6**, 226 (2018).
21. M. S. Zinter, M. Y. Mayday, K. K. Ryckman, L. L. Jelliffe-Pawlowski, J. L. DeRisi, Towards precision quantification of contamination in metagenomic sequencing experiments. *Microbiome* **7**, 62 (2019).
22. P. P. Bosshard, R. Zbinden, M. Altwegg, *Paenibacillus turicensis* sp. nov., a novel bacterium harbouring heterogeneities between 16S rRNA genes. *Int. J. Syst. Evol. Microbiol.* **52**, 2241–2249 (2002).
23. S. D. DeLeon, R. C. Welliver Sr., *Paenibacillus alvei* sepsis in a neonate. *Pediatr. Infect. Dis. J.* **35**, 358 (2016).
24. V. Roux, L. Fenner, D. Raoult, *Paenibacillus provencensis* sp. nov., isolated from human cerebrospinal fluid, and *Paenibacillus urinalis* sp. nov., isolated from human urine. *Int. J. Syst. Evol. Microbiol.* **58**, 682–687 (2008).
25. Y. Kuno, *Bacillus thiaminolyticus*, a new thiamin-decomposing bacterium. *Imp. Acad. Japan Proc.* **27**, 362–365 (1951).
26. J. Ouyang, Z. Pei, L. Lutwick, S. Dalal, L. Yang, N. Cassai, K. Sandhu, B. Hanna, R. L. Wieczorek, M. Bluth, M. R. Pincus, *Paenibacillus thiaminolyticus*: A new cause of human infection, inducing bacteremia in a patient on hemodialysis. *Ann. Clin. Lab. Sci.* **38**, 393–400 (2008).

27. N. Latt, G. Dore, Thiamine in the treatment of Wernicke encephalopathy in patients with alcohol use disorders. *Intern. Med. J.* **44**, 911–915 (2014).
28. D. Lonsdale, A review of the biochemistry, metabolism and clinical benefits of thiamin(e) and its derivatives. *Evid. Based Complement. Alternat. Med.* **3**, 49–59 (2006).
29. K. E. Milad, G. S. Ridha, The occurrence of thiamine-responsive polioencephalomalacia in dromedary breeding camels in Libya: Preliminary investigation of diagnosis. *Iraqi J. Vet. Sci.* **23** (suppl. 1), 119–122 (2009).
30. D. Coats, K. Shelton-Dodge, K. Ou, V. Khun, S. Seab, K. Sok, C. Prou, S. Tortorelli, T. P. Moyer, L. E. Cooper, T. P. Begley, F. Enders, P. R. Fischer, M. Topazian, Thiamine deficiency in Cambodian infants with and without beriberi. *J. Pediatr.* **161**, 843–847 (2012).
31. L. Hiffler, B. Rakotoambinina, N. Lafferty, D. Martinez Garcia, Thiamine deficiency in tropical pediatrics: New insights into a neglected but vital metabolic challenge. *Front. Nutr.* **3**, 16 (2016).
32. C. A. Richter, A. N. Evans, M. K. Wright-Osment, J. L. Zajicek, S. A. Heppell, S. C. Riley, C. C. Krueger, D. E. Tillitt, *Paenibacillus thiaminolyticus* is not the cause of thiamine deficiency impeding lake trout (*Salvelinus namaycush*) recruitment in the Great Lakes. *Can. J. Fish. Aquat. Sci.* **69**, 1056–1064 (2012).
33. A. Louveau, T. H. Harris, J. Kipnis, Revisiting the mechanisms of CNS immune privilege. *Trends Immunol.* **36**, 569–577 (2015).
34. C. Menendez, A. Mayor, Congenital malaria: The least known consequence of malaria in pregnancy. *Semin. Fetal Neonatal Med.* **12**, 207–213 (2007).
35. J.-L. Casanova, Severe infectious diseases of childhood as monogenic inborn errors of immunity. *Proc. Natl. Acad. Sci. U.S.A.* **112**, E7128–E7137 (2015).
36. N. J. Afacan, C. D. Fjell, R. E. Hancock, A systems biology approach to nutritional immunology—Focus on innate immunity. *Mol. Aspects Med.* **33**, 14–25 (2012).
37. R. Koch, An address on bacteriological research. *Br. Med. J.* **2**, 380–383 (1890).
38. D. N. Fredericks, D. A. Relman, Sequence-based identification of microbial pathogens: A reconsideration of Koch's postulates. *Clin. Microbiol. Rev.* **9**, 18–33 (1996).
39. C. P. Skipper, M. R. Schleiss, A. S. Bangdiwala, N. Hernandez-Alvarado, K. Taseera, H. W. Nabeta, A. K. Musubire, S. M. Lofgren, D. L. Wiesner, J. Rhein, R. Rajasingham, C. Schutz, G. Meintjes, C. Muzoora, D. B. Meya, D. R. Boulware; Cryptococcal Optimal Antiretroviral Therapy Timing (COAT) Team, Cytomegalovirus viremia associated with increased mortality in cryptococcal meningitis in sub-Saharan Africa. *Clin. Infect. Dis.* **71**, 525–531 (2020).
40. C. C. Moore, S. T. Jacob, P. Banura, J. Zhang, S. Stroup, D. R. Boulware, W. M. Scheld, E. R. Houpt, J. Liu, Etiology of sepsis in Uganda using a quantitative polymerase chain reaction-based TaqMan Array Card. *Clin. Infect. Dis.* **68**, 266–272 (2019).
41. A. H. Walton, J. T. Muenzer, D. Rasche, J. S. Boomer, B. Sato, B. H. Brownstein, A. Pachot, T. L. Brooks, E. Deych, W. D. Shannon, J. M. Green, G. A. Storch, R. S. Hotchkiss, Reactivation of multiple viruses in patients with sepsis. *PLOS ONE* **9**, e98819 (2014).
42. G. Monneret, F. Venet, Sepsis-induced immune alterations monitoring by flow cytometry as a promising tool for individualized therapy. *Cytometry B Clin. Cytom.* **90**, 376–386 (2016).
43. W. G. Nichols, L. Corey, T. Gooley, C. Davis, M. Boeckh, High risk of death due to bacterial and fungal infection among cytomegalovirus (CMV)—Seronegative recipients of stem cell transplants from seropositive donors: Evidence for indirect effects of primary CMV infection. *J. Infect. Dis.* **185**, 273–282 (2002).
44. S. J. Schiff, S. L. Ranjeva, T. D. Sauer, B. C. Warf, Rainfall drives hydrocephalus in East Africa. *J. Neurosurg. Pediatr.* **10**, 161–167 (2012).
45. W. J. Wiersinga, H. S. Virk, A. G. Torres, B. J. Currie, S. J. Peacock, D. A. B. Dance, D. Limmathurotsakul, Melioidosis. *Nat. Rev. Dis. Primers* **4**, 17107 (2018).
46. T. E. Chao, K. Sharma, M. Mandigo, L. Hagander, S. C. Resch, T. G. Weiser, J. G. Meara, Cost-effectiveness of surgery and its policy implications for global health: A systematic review and analysis. *Lancet Glob. Health* **2**, e334–e345 (2014).
47. J. G. Caporaso, J. Kuczynski, J. Stombaugh, K. Bittinger, F. D. Bushman, E. K. Costello, N. Fierer, A. G. Peña, J. K. Goodrich, J. I. Gordon, G. A. Huttley, S. T. Kelley, D. Knights, J. E. Koenig, R. E. Ley, C. A. Lozupone, D. McDonald, B. D. Muegge, M. Pirrung, J. Reeder, J. R. Sevinsky, P. J. Turnbaugh, W. A. Walters, J. Widmann, T. Yatsunenko, J. Zaneveld, R. Knight, QIIME allows analysis of high-throughput community sequencing data. *Nat. Methods* **7**, 335–336 (2010).
48. J. N. Paulson, O. C. Stine, H. C. Bravo, M. Pop, Differential abundance analysis for microbial marker-gene surveys. *Nat. Methods* **10**, 1200–1202 (2013).
49. C. Ruehl-Fehlert, B. Kittel, G. Morawietz, P. Deslex, C. Keenan, C. R. Mahrt, T. Nolte, M. Robinson, B. P. Stuart, U. Deschl; RITA Group; NACAD Group, Revised guides for organ sampling and trimming in rats and mice–part 1: A joint publication of the RITA and NACAD groups. *Exp. Toxicol. Pathol.* **55**, 91–106 (2003).
50. B. Kittel, C. Ruehl-Fehlert, G. Morawietz, J. Klapwijk, M. R. Elwell, B. Lenz, M. G. O'Sullivan, D. R. Roth, P. F. Wadsworth; RITA Group; NACAD Group, Revised guides for organ sampling and trimming in rats and mice–Part 2: A joint publication of the RITA and NACAD groups. *Exp. Toxicol. Pathol.* **55**, 413–431 (2004).
51. G. Morawietz, C. Ruehl-Fehlert, B. Kittel, A. Bube, K. Keane, S. Halm, A. Heuser, J. Hellmann; RITA Group; NACAD Group, Revised guides for organ sampling and trimming in rats and mice–Part 3. A joint publication of the RITA and NACAD groups. *Exp. Toxicol. Pathol.* **55**, 433–449 (2004).
52. Y. Benjamini, Y. Hochberg, Controlling the false discovery rate: A practical and powerful approach to multiple testing. *J. R. Stat. Soc. Ser. B Stat. Methodol.* **57**, 289–300 (1995).
53. C. Ash, F. G. Priest, M. D. Collins, Molecular identification of rRNA group 3 bacilli (Ash, Farrow, Wallbanks and Collins) using a PCR probe test. Proposal for the creation of a new genus *Paenibacillus*. *Antonie Van Leeuwenhoek* **64**, 253–260 (1993).
54. J. G. Caporaso, C. L. Lauber, W. A. Walters, D. Berg-Lyons, J. Huntley, N. Fierer, S. M. Owens, J. Betley, L. Fraser, M. Bauer, N. Gormley, J. A. Gilbert, G. Smith, R. Knight, Ultra-high-throughput microbial community analysis on the Illumina HiSeq and MiSeq platforms. *ISME J.* **6**, 1621–1624 (2012).
55. S.-S. Chang, H.-L. Hsu, J.-C. Cheng, C.-P. Tseng, An efficient strategy for broad-range detection of low abundance bacteria without DNA decontamination of PCR reagents. *PLOS ONE* **6**, e20303 (2011).
56. N. D. Olson, N. Shah, J. Kancherla, J. Wagner, J. N. Paulson, H. Corrada-Bravo, *metagenomeFeatures*: An R package for working with 16S rRNA reference databases and marker-gene survey feature data. *Bioinformatics* **35**, 3870–3872 (2019).
57. N. D. Olson, J. N. Paulson, H. Corrada-Bravo, (2018). greengenes13.5MgDb: Greengenes 13.5 16S rRNA Database Annotation Data. R package version 2.0.0, https://bioconductor.org/packages/greengenes13.5MgDb/ 10.18129/B9.bioc.greengenes13.5MgDb
58. T. Z. DeSantis, P. Hugenholtz, N. Larsen, M. Rojas, E. L. Brodie, K. Keller, T. Huber, D. Dalevi, P. Hu, G. L. Andersen, Greengenes, a chimera-checked 16S rRNA gene database and workbench compatible with ARB. *Appl. Environ. Microbiol.* **72**, 5069–5072 (2006).
59. B. J. Haas, D. Gevers, A. M. Earl, M. Feldgarden, D. V. Ward, G. Giannoukos, D. Ciulla, D. Tabbaa, S. K. Highlander, E. Sodergren, B. Methé, T. Z. DeSantis; Human Microbiome Consortium, J. F. Petrosino, R. Knight, B. W. Birren, Chimeric 16S rRNA sequence formation and detection in Sanger and 454-pyrosequenced PCR amplicons. *Genome Res.* **21**, 494–504 (2011).
60. Q. Wang, G. M. Garrity, J. M. Tiedje, J. R. Cole, Naive Bayesian classifier for rapid assignment of rRNA sequences into the new bacterial taxonomy. *Appl. Environ. Microbiol.* **73**, 5261–5267 (2007).
61. A. Bankevich, S. Nurk, D. Antipov, A. A. Gurevich, M. Dvorkin, A. S. Kulikov, V. M. Lesin, S. I. Nikolenko, S. Pham, A. D. Prjibelski, A. V. Pyshkin, A. V. Sirotkin, N. Vyahhi, G. Tesler, M. A. Alekseyev, P. A. Pevzner, SPAdes: A new genome assembly algorithm and its applications to single-cell sequencing. *J. Comput. Biol.* **19**, 455–477 (2012).
62. B. J. Walker, T. Abeel, T. Shea, M. Priest, A. Abouelliel, S. Sakthikumar, C. A. Cuomo, Q. Zheng, J. Wortman, S. K. Young, A. M. Earl, Pilon: an integrated tool for comprehensive microbial variant detection and genome assembly improvement.. *PLoS One* **9**, e112963 (2014).
63. S. Koren, B. P. Walenz, K. Berlin, J. R. Miller, N. H. Bergman, A. M. Phillippy, Canu: Scalable and accurate long-read assembly via adaptive *k*-mer weighting and repeat separation. *Genome Res.* **27**, 722–736 (2017).
64. M. Nei, S. Kumar, *Molecular Evolution and Phylogenetics* (Oxford Univ. Press, 2000), pp. 333.
65. N. Saitou, M. Nei, The neighbor-joining method: A new method for reconstructing phylogenetic trees. *Mol. Biol. Evol.* **4**, 406–425 (1987).
66. J. Felsenstein, Confidence limits on phylogenies: An approach using the bootstrap. *Evolution* **39**, 783–791 (1985).
67. M. Kimura, A simple method for estimating evolutionary rates of base substitutions through comparative studies of nucleotide sequences. *J. Mol. Evol.* **16**, 111–120 (1980).
68. C. Quast, E. Pruesse, P. Yilmaz, J. Gerken, T. Schweer, P. Yarza, J. Peplies, F. O. Glöckner, The SILVA ribosomal RNA gene database project: Improved data processing and web-based tools. *Nucleic Acids Res.* **41**, D590–D596 (2013).
69. S. F. Altschul, W. Gish, W. Miller, E. W. Myers, D. J. Lipman, Basic local alignment search tool. *J. Mol. Biol.* **215**, 403–410 (1990).
70. D. Hyatt, G.-L. Chen, P. F. Locascio, M. L. Land, F. W. Larimer, L. J. Hauser, Prodigal: Prokaryotic gene recognition and translation initiation site identification. *BMC Bioinformatics* **11**, 119 (2010).
71. J. R. Kultima, S. Sunagawa, J. Li, W. Chen, H. Chen, D. R. Mende, M. Arumugam, Q. Pan, B. Liu, J. Qin, J. Wang, P. Bork, MOCAT: A metagenomics assembly and gene prediction toolkit. *PLOS ONE* **7**, e47656 (2012).
72. R. C. Edgar, MUSCLE: A multiple sequence alignment method with reduced time and space complexity. *BMC Bioinformatics* **5**, 113 (2004).
73. M. N. Price, P. S. Dehal, A. P. Arkin, FastTree 2–approximately maximum-likelihood trees for large alignments. *PLOS ONE* **5**, e9490 (2010).
74. I. Letunic, P. Bork, Interactive tree of life (iTOL) v3: An online tool for the display and annotation of phylogenetic and other trees. *Nucleic Acids Res.* **44**, W242–W245 (2016).
75. A. R. Wattam, D. Abraham, O. Dalay, T. L. Disz, T. Driscoll, J. L. Gabbard, J. J. Gillespie, R. Gough, D. Hix, R. Kenyon, D. Machi, C. Mao, E. K. Nordberg, R. Olson, R. Overbeek, G. D. Pusch, M. Shukla, J. Schulman, R. L. Stevens, D. E. Sullivan, V. Vonstein, A. Warren,

R. Will, M. J. Wilson, H. S. Yoo, C. Zhang, Y. Zhang, B. W. Sobral, PATRIC, the bacterial bioinformatics database and analysis resource. *Nucleic Acids Res.* **42**, D581–D591 (2014).
76. L. Zammarchi, M. G. Colao, A. Mantella, T. Capobianco, G. Mazzarelli, N. Ciccone, S. Tekle Kiros, E. Mantengoli, G. M. Rossolini, A. Bartoloni, Evaluation of a new rapid fluorescence immunoassay for the diagnosis of dengue and Zika virus infection. *J. Clin. Virol.* **112**, 34–39 (2019).
77. B. Langmead, S. L. Salzberg, Fast gapped-read alignment with Bowtie 2. *Nat. Methods* **9**, 357–359 (2012).
78. B. Chevreux, T. Pfisterer, B. Drescher, A. J. Driesel, W. E. Müller, T. Wetter, S. Suhai, Using the miraEST assembler for reliable and automated mRNA transcript assembly and SNP detection in sequenced ESTs. *Genome Res.* **14**, 1147–1159 (2004).
79. B. Zweygberg Wirgart, M. Brytting, A. Linde, B. Wahren, L. Grillner, Sequence variation within three important cytomegalovirus gene regions in isolates from four different patient populations. *J. Clin. Microbiol.* **36**, 3662–3669 (1998).
80. W. Habbal, F. Monem, B. C. Gärtner, Comparative evaluation of published cytomegalovirus primers for rapid real-time PCR: Which are the most sensitive? *J. Med. Microbiol.* **58**, 878–883 (2009).
81. M. Lopper, T. Compton, Disulfide bond configuration of human cytomegalovirus glycoprotein B. *J. Virol.* **76**, 6073–6082 (2002).
82. M. K. Isaacson, T. Compton, Human cytomegalovirus glycoprotein B is required for virus entry and cell-to-cell spread but not for virion attachment, assembly, or egress. *J. Virol.* **83**, 3891–3903 (2009).
83. J. L. Sanchez, G. A. Storch, Multiplex, quantitative, real-time PCR assay for cytomegalovirus and human DNA. *J. Clin. Microbiol.* **40**, 2381–2386 (2002).
84. B. Ewing, L. Hillier, M. C. Wendl, P. Green, Base-calling of automated sequencer traces using phred. I. Accuracy assessment. *Genome Res.* **8**, 175–185 (1998).
85. B. Ewing, P. Green, Base-calling of automated sequencer traces using phred.II. Error probabilities. *Genome Res.* **8**, 186–194 (1998).
86. A. M. Bolger, M. Lohse, B. Usadel, Trimmomatic: A flexible trimmer for Illumina sequence data. *Bioinformatics* **30**, 2114–2120 (2014).
87. H. Li, B. Handsaker, A. Wysoker, T. Fennell, J. Ruan, N. Homer, G. Marth, G. Abecasis, R. Durbin; 1000 Genome Project Data Processing Subgroup, The Sequence alignment/Map format and SAMtools. *Bioinformatics* **25**, 2078–2079 (2009).
88. G. Benson, Tandem repeats finder: A program to analyze DNA sequences. *Nucleic Acids Res.* **27**, 573–580 (1999).
89. P. Ssentongo, A. J. B. Muwanguzi, U. Eden, T. Sauer, G. Bwanga, G. Kateregga, L. Aribo, M. Ojara, W. K. Mugerwa, S. J. Schiff, Changes in Ugandan climate rainfall at the village and forest level. *Sci. Rep.* **8**, 3551 (2018).
90. B. Flury, *A First Course in Multivariate Statistics* (Springer Texts in Statistics, Springer, 1997).
91. M. Rougemont, M. Van Saanen, R. Sahli, H. P. Hinrikson, J. Bille, K. Jaton, Detection of four *Plasmodium* species in blood from humans by 18S rRNA gene subunit-based and species-specific real-time PCR assays. *J. Clin. Microbiol.* **42**, 5636–5643 (2004).
92. J. L. Burg, C. M. Grover, P. Pouletty, J. C. Boothroyd, Direct and sensitive detection of a pathogenic protozoan, Toxoplasma gondii, by polymerase chain reaction. *J. Clin. Microbiol.* **27**, 1787–1792 (1989).
93. M. Kabiri, D. Steverding, Studies on the recycling of the transferrin receptor in *Trypanosoma brucei* using an inducible gene expression system. *Eur. J. Biochem.* **267**, 3309–3314 (2000).
94. D. R. Moser, L. V. Kirchhoff, J. E. Donelson, Detection of Trypanosoma cruzi by DNA amplification using the polymerase chain reaction. *J. Clin. Microbiol.* **27**, 1477–1482 (1989).
95. R. Campos-Herrera, F. E. El-Borai, R. J. Stuart, J. H. Graham, L. W. Duncan, Entomopathogenic nematodes, phoretic Paenibacillus spp., and the use of real time quantitative PCR to explore soil food webs in Florida citrus groves. *J Invertebr Pathol* **108**, 30–39 (2011).
96. T. Z. DeSantis, E. L. Brodie, J. P. Moberg, I. X. Zubieta, Y. M. Piceno, G. L. Andersen, High-density universal 16S rRNA microarray analysis reveals broader diversity than typical clone library when sampling the environment. *Microb. Ecol.* **53**, 371–383 (2007).
97. M. A. Tanner, B. M. Goebel, M. A. Dojka, N. R. Pace, Specific ribosomal DNA sequences from diverse environmental settings correlate with experimental contaminants. *Appl. Environ. Microbiol.* **64**, 3110–3113 (1998).
98. T. J. White, T. D. Bruns, S. B. Lee, J. W. Taylor, *PCR—Protocols and Applications—A Laboratory Manual* (Academic Press, 1990), pp. 315–322.
99. S. Weidner, W. Arnold, A. Puhler, Diversity of uncultured microorganisms associated with the seagrass Halophila stipulacea estimated by restriction fragment length polymorphism analysis of PCR-amplified 16S rRNA genes. *Appl. Environ. Microbiol.* **62**, 766–771 (1996).
100. M. E. Ritchie, B. Phipson, D. Wu, Y. Hu, C. W. Law, W. Shi, G. K. Smyth, *limma* powers differential expression analyses for RNA-sequencing and microarray studies. *Nucleic Acids Res.* **43**, e47 (2015).

Acknowledgments: We thank N. D. Olson, A. Patterson, Q. Liu, M. Mwebingwa, M. Poss, V. Kapur, and D. Craft for helpful discussions and K. Moran for technical assistance. **Funding:** This study was supported by NIH Director's Pioneer Award 1DP1HD086071 and NIH Director's Transformative Award 1R01AI145057. J.N.P. was supported as a consultant for work on this project from NIH grants 1DP1HD086071 and 1R01AI145057. J.E.E. was supported by National Center for Advancing Translational Sciences grant #KL2 TR002015. M.Y.G. was supported by the NIH Intramural Research Program at the National Library of Medicine. A.D.W. received salary support through an in-kind contribution from the University of Liverpool. **Author contributions:** Bacteriology was carried out by D.S.S.W., B.v.B., and J.B. with help from M.Y.G. and M.A. Virology was performed by N.M. Wet lab technical analysis was performed by C.H., M.C.-R., C.G., and J.N. Animal experiments were carried out by P.Ssentongo, and histology was performed by H.A. Clinical work was performed by J. Mugamba, F.B., E.M.-K., R.M., E.K., J. Magombe, P. O.-O., J. O., K.B., and P. Ssenyonga. Bioinformatics was performed by J.N.P., L.Z., F.R., and J.Q. Neurosurgical consultation was performed by A.V.K., D.D.L., B.C.W., and S.J.S. Infectious disease consultation was provided by L.M.B. and J.E.E. Computer support was performed by B.N.K. Immunology consultation was performed by S.U.M. and M. Hornig. Proteomics on CSF samples was performed by A.M.I., R.T., and D.D.L. Statistical analysis was performed by J.N.P., M. Haran, and X.L., and geographical mapping was performed by A.J.W. and P. Ssentongo. Data analysis was performed by J.N.P., B.L.W., C.H., N.M., L.Z., S.M.K., M.R.P., and S.J.S. J.N.P., B.L.W., and C.H. wrote the paper, and all authors contributed to editing the manuscript. **Competing interests:** N.M. has consulted for Third Bridge and Summerbio. D.D.L. has received research support from Microbot Medical Inc. and Medtronic Inc. W.I.L. has consulting agreements with Amazon, Deerfield Health, Democratic National Committee, Directors Guild of America, Pandefense, Pfizer, and Virgin. A.V.K. has consulted for Medtronic Inc. J.E.E. consults for Allergan. M.G. consults for UNICEF Uganda, Laterite (Rwanda), COWI (Mozambique), New York University, Boston University, and the World Health Organization. M.F. consults for Epicentre/MSF and WHO SAGE Measles and Rubella Working Group. **Data and materials availability:** All data associated with this study are in the main text or the Supplementary Materials. The assembled genome of *P. thiaminolyticus* Mbale strain has been deposited in GenBank with accession number CP041404. Sequencing data for bacterial 16*S* rDNA, in silico host-depleted mRNA, and VirCapSeq data, along with sample metadata, are available at the NCBI archive under project ID #PRJNA605220. Processed data, including counts and relative abundance for taxa, along with sample metadata, are available at MicrobiomeDB.org under the dataset record number DS_953b8ff2d4. There is a materials transfer agreement between the CURE Children's Hospital of Uganda and Mbarara University of Science and Technology, with Penn State University as the recipient. The parties jointly own rights to *P. thiaminolyticus* Mbale and will share in any commercialization of the research on this organism. The *P. thiaminolyticus* Mbale strain will be deposited in a publicly accessible repository once the safety of this organism has been determined.

Submitted 31 October 2019
Accepted 6 May 2020
Published 30 September 2020
10.1126/scitranslmed.aba0565

Citation: J. N. Paulson, B. L. Williams, C. Hehnly, N. Mishra, S. A. Sinnar, L. Zhang, P. Ssentongo, E. Mbabazi-Kabachelor, D. S. S. Wijetunge, B. von Bredow, R. Mulondo, J. Kiwanuka, F. Bajunirwe, J. Bazira, L. M. Bebell, K. Burgoine, M. Couto-Rodriguez, J. E. Ericson, T. Erickson, M. Ferrari, M. Gladstone, C. Guo, M. Haran, M. Hornig, A. M. Isaacs, B. N. Kaaya, S. M. Kangere, A. V. Kulkarni, E. Kumbakumba, X. Li, D. D. Limbrick Jr., J. Magombe, S. U. Morton, J. Mugamba, J. Ng, P. Olupot-Olupot, J. Onen, M. R. Peterson, F. Roy, K. Sheldon, R. Townsend, A. D. Weeks, A. J. Whalen, J. Quackenbush, P. Ssenyonga, M. Y. Galperin, M. Almeida, H. Atkins, B. C. Warf, W. I. Lipkin, J. R. Broach, S. J. Schiff, *Paenibacillus* infection with frequent viral coinfection contributes to postinfectious hydrocephalus in Ugandan infants. *Sci. Transl. Med.* **12**, eaba0565 (2020).

Science Translational Medicine

Paenibacillus infection with frequent viral coinfection contributes to postinfectious hydrocephalus in Ugandan infants

Joseph N. Paulson, Brent L. Williams, Christine Hehnly, Nischay Mishra, Shamim A. Sinnar, Lijun Zhang, Paddy Ssentongo, Edith Mbabazi-Kabachelor, Dona S. S. Wijetunge, Benjamin von Bredow, Ronnie Mulondo, Julius Kiwanuka, Francis Bajunirwe, Joel Bazira, Lisa M. Bebell, Kathy Burgoine, Mara Couto-Rodriguez, Jessica E. Ericson, Tim Erickson, Matthew Ferrari, Melissa Gladstone, Cheng Guo, Murali Haran, Mady Hornig, Albert M. Isaacs, Brian Nsubuga Kaaya, Sheila M. Kangere, Abhaya V. Kulkarni, Elias Kumbakumba, Xiaoxiao Li, David D. Limbrick, Jr., Joshua Magombe, Sarah U. Morton, John Mugamba, James Ng, Peter Olupot-Olupot, Justin Onen, Mallory R. Peterson, Farrah Roy, Kathryn Sheldon, Reid Townsend, Andrew D. Weeks, Andrew J. Whalen, John Quackenbush, Peter Ssenyonga, Michael Y. Galperin, Mathieu Almeida, Hannah Atkins, Benjamin C. Warf, W. Ian Lipkin, James R. Broach and Steven J. Schiff

Sci Transl Med **12**, eaba0565.
DOI: 10.1126/scitranslmed.aba0565

Hiding in plain sight

Hydrocephalus is a serious brain disorder in children and the most common indication for pediatric neurosurgery. Worldwide, the most frequent cause of hydrocephalus is previous infection such as neonatal sepsis. Such postinfectious hydrocephalus (PIH) occurs principally in low- and middle-income countries, and the pathogens responsible remain uncharacterized. Paulson *et al.* used pan-microbial analysis of CSF samples from infants with PIH in Uganda to identify the bacteria, viruses, fungi, or parasites potentially contributing to PIH. They found a new strain of the bacterium *Paenibacillus* as well as frequent coinfection with cytomegalovirus as contributors to PIH in this infant cohort.